Stage-dependent changes in oviductal phospholipid profiles throughout the estrous cycle in cattle

Charles Banliat, Daniel Tomas, Ana-Paula Teixeira-Gomes, Svetlana Uzbekova, Benoît Guyonnet, Valérie Labas, Marie Saint-Dizier

Title: Stage-dependent changes in oviductal phospholipid profiles throughout the estrous cycle in cattle

Authors' names and affiliations: Charles Banliat[a,b], Daniel Tomas[a,c], Ana-Paula Teixeira-Gomes[c,d], Svetlana Uzbekova[a], Benoît Guyonnet[b], Valérie Labas[a,c] and Marie Saint-Dizier[a,e]

[a]UMR PRC, INRA 85, CNRS 7247, University of Tours, IFCE, 37380 Nouzilly, France

[b]Union Evolution, rue Eric Tabarly CS10040, 35538 Noyal-Sur-Vilaine, France

[c]Plate-forme de Chirurgie et d'Imagerie pour la Recherche et l'Enseignement (CIRE), Pôle d'Analyse et d'Imagerie des Biomolécules (PAIB), INRA, CHRU of Tours, University of Tours, 37380 Nouzilly, France.

[d]UMR ISP, INRA 1282, University of Tours, 37380 Nouzilly, France

[e]University of Tours, Faculty of Sciences and Techniques, 37200 Tours, France

Corresponding author: Marie Saint-Dizier, University of Tours, Faculty of Sciences and Techniques, Parc de Grandmont, 37200 Tours, France; Tel : +33 247367014; Fax : +33 247367094; Email: marie.saint-dizier@univ-tours.fr

Abstract

Sperm capacitation, fertilization and embryo development take place in the oviduct during the periovulatory period of the estrous cycle. Phospholipids are crucial metabolites for sperm capacitation and early embryo development. The aim of this study was to monitor the abundance of phospholipids in the bovine oviductal fluid (OF) according to the stage of the estrous cycle and the side relative to ovulation. Pairs of bovine oviducts were collected in a slaughterhouse and classified into four stages of the estrous cycle: post-ovulatory (Post-ov), mid-luteal (Mid-lut), late-luteal (Late-lut) and pre-ovulatory (Pre-ov) phases (n = 17 cows/stage). Cell-free OF from oviducts ipsilateral and contralateral to the site of ovulation were analyzed using MALDI-TOF mass spectrometry. Lipid identification was achieved by high resolution mass spectrometry. A total of 274 lipid masses were detected in the mass range of 400-1000 Da, corresponding mostly to phosphatidylcholines (PC), lysoPC, phosphatidylethanolamine (PE), lysoPE and sphingomyelins (SM). Ipsilateral and contralateral OF did not differ in their lipid profiles at any stage of the cycle. However, 127 and 96 masses were differentially abundant between stages in ipsilateral and contralateral OF, respectively. Highest differences in lipid profiles were observed in the Pre-ov *vs*. Mid-lut and Pre-ov *vs*. Late-lut comparisons in both sides relative to ovulation. Differential abundance of specific molecules of PC, PE, SM and L-carnitine were observed at Pre-ov and Post-ov compared with the luteal phase. This work proposes new candidates potentially able to regulate sperm capacitation and early embryo development.

Key words: Bovine, oviduct fluid, estrus cycle, phospholipids, sphingolipids; MALDI-TOF mass spectrometry.

1. Introduction

The mammalian oviductal fluid (OF) is a complex and changing fluid resulting from the secretion of oviduct luminal epithelial cells, transudate from the circulating blood and presumably compounds from the follicular fluid at the time of ovulation [1, 2]. Gamete final maturation, fertilization and early embryo development take place in this dynamic fluid environment. However, the composition and physiological factors regulating the OF have been poorly investigated [3]. The OF contains a variety of lipids including fatty acids, triglycerides, cholesterol and phospholipids [4-6]. Glycerophospholipids and sphingolipids are vital energy substrates acting as structural and regulatory components of cell membranes and extracellular microvesicles [7-9]. In addition, a number of phosphatidylcholines (PC) and sphingomyelins (SM) are lipid mediators implied in many cell signaling pathways and act as crucial precursors of many biomolecules such as lysophospholipids (LPC) and prostaglandins [7].

After entering the oviduct, spermatozoa must accomplish capacitation to fertilize. Exogenous phospholipids and cholesterol have been reported to be taken up by spermatozoa, influencing sperm capacitation and ability to undergo acrosome reaction and fertilize the oocyte [10, 11]. After fertilization, developing embryos up to the blastocyst stage undergo important changes in their phospholipid composition [12]. There is evidence from *in vivo* and *in vitro* studies that the lipid environment to which early bovine embryos are exposed has a significant impact on their quality in terms of morphology, post-cryopreservation survival, lipidomic and transcriptomic signatures [13-16].

It is assumed that the oviductal secretions provide an optimal environment for sperm capacitation, fertilization and embryo development leading to the establishment of pregnancy. However, the specific requirements in lipid metabolism of gametes and embryo imply significant regulation in oviductal secretions between the periovulatory period and the luteal

phase of the cycle. In mono-ovular species, the side of ovulation may also affect the molecular composition of the proximal OF by topical hormonal regulations and putative input of the ovulatory follicle. Previously, we reported important fluctuations in the levels of steroid hormones, metabolites and proteins in the bovine OF according to the stage of estrous cycle and the side relative to ovulation [17-19]. The ovarian steroid hormones progesterone (P4) and 17β-estradiol (E2) play important regulatory roles in the secretory activity of the oviduct epithelium [17, 18, 20]. However, information on the lipid content of the oviduct is scarce. Only four studies on material from no more than four animals per study reported changes in the phospholipid content of the bovine OF across the cycle with no distinction between sides of ovulation nor between lipid species [4, 5, 21, 22]. A recent study reported the phospholipid profiles in uterine and oviductal tissues from zebuine females [23]. However, this study focused only on the early luteal (or post-ovulatory) phase of the estrous cycle in the ipsilateral oviduct.

The objectives of this study was thus to monitor the diversity and abundance of lipids in the bovine OF according to the stage of the estrous cycle and the side relative to ovulation. The MALDI-TOF (Matrix assisted laser desorption ionization - Time of flight) mass spectrometry (MALDI-MS) was used because it is largely recognized as a powerful, rapid and sensitive way to obtain lipid profiles in a relatively large range of molecular weights without requiring prior lipid extraction. For precise lipid identification, complementary tandem high-resolution mass spectrometry (HR-MS/MS) was applied.

2. Materials and Methods

2.1. Collection of bovine oviductal fluids

Both oviducts and ovaries from adult *Bos Taurus* cows were collected at a local slaughterhouse (Vendôme, France), placed on ice within 15 min after death and transported to the laboratory (40-min transportation). Oviducts were classified into four stages in the estrous cycle according to the morphology of ovaries, as previously described (Ireland et al 1980): post-ovulatory (Post-ov), mid luteal (Mid-lut), late luteal (Late-lut) and pre-ovulatory (Pre-ov) stages of the estrous cycle (N=17 cows/stage). To avoid the inclusion of cows with cystic follicles in the Pre-ov group, animals with a Pre-ov follicle larger than 20 mm in diameter (>2.4 mL of follicular fluid) and/or with intra-follicular P4 concentrations higher than 160 ng/mL (as measured by a competitive enzyme-linked immunosorbent assay [24]) were not included. The OF and epithelial cells were collected from the whole ipsilateral (to corpus luteum or Pre-ov follicle) and contralateral oviducts by gentle squeezing with a glass slide. Mixtures were stored on ice then OF was separated from the cells and cellular debris by two centrifugations (2000 g, 15 min then 12 000 g, 10 min) at 4°C. The OF collected (20-100 µl per oviduct) was immediately stored in liquid nitrogen to preclude any lipid degradation before analysis. The whole processing time from animal death up to sample storage was less than 4 hours.

2.2. Lipid profiling by MALDI-TOF mass spectrometry (MALDI-MS)

Lipid profiling of OF samples was performed as previously described for bovine follicular fluid [25] with slight modifications. Briefly, the samples were thawed and sonicated on ice for 10 min. Then, 0.5 µL of OF was spotted on the TP Ground Steel 384 MALDI plate (Bruker Daltonics, Bremen, Germany), dried at room temperature for 30 minutes then overlaid with 2 µL of 2,4,6-trihydroxyacetophenone (THAP) matrix at 10 mg/mL solubilized in 90% methanol and 0.2% (w/v) trifluoroacetic acid (TFA) and containing 0.001 mg/mL of phosphatidylcholine (PC 20:0, m/z 604.3375; Sigma P7081) as internal standard (not initially present in the OF). The sample/matrix mixtures were then dried at room temperature for 30

min. For each sample, five technical replicates were spotted. Spectra were acquired with an UltrafleXtreme MALDI-TOF instrument (Bruker Daltonics, Bremen, Germany) equipped with a Smartbeam laser at 2 kHz laser repetition controlled by flexControl 3.4 software (Bruker Daltonics, Bremen, Germany). A total of 10 spectra per sample (2 spectra per technical replicate, 5000 shots per spectra) were acquired in the positive reflectron ion mode in the mass/charge (m/z) range of 100-1200. External calibration was performed using a mixture of caffein, MRFA peptide, leu-enkephalin, bradykinine 2-9 and glu1-fibrinopeptide at 1 mM each, 1.64 mM of reserpine, 942 µM of bradykinine and 771 µM of angiotensine in 1 µL of α-cyano-4-hydroxycinnamic acid (CHCA, 20 mg/mL) solubilized in 50% acetonitrile and 0.1% (w/v) TFA. To increase the mass accuracy (mass error <0.05%), an internal calibration using a lock mass at m/z 604.3375 corresponding to PC 20:0 was subsequently applied to all spectra by flexAnalysis 3.4 software (Bruker Daltonics), as previously described [25]. The data were integrated in the R software (version 3.5.0) and treated for baseline subtraction using the Statistics-sensitive Non-linear Iterative Peak-clipping algorithm (SNIP, minimum 15 iterations), smoothing (Savitzky-Golay algorithm, m/z range = 0.1), spectra alignment using prominent peaks (difference between spectra < 0.002%) and normalization on intensity using total ion count (TIC).

Peaks were detected using a total average spectrum with a signal/background noise > 2 in the mass range of 400-1000 m/z. The different isotopes of a given mass were not considered for analysis. The coefficient of variation (CV%) of intensity values (normalized peak height, NPH) was calculated for all the peaks in 10 technical replicates per sample, from 17 different OF for each stage and side. The mean CV% of the normalized peak intensity values was less than 25 %.

2.3. Analysis of MALDI-MS data

Statistical analyses were performed using the MALDIquant and MALDIquantForeign packages (v 1.17 & v0.11.1) of the R software (version 3.5.0) [26]. MS data did not pass the Kolmogorov-Smirnov's test of normality. All lipidomic data without preselection were submitted to the non-parametric Wilcoxon test to identify changes between sides of ovulation and to the Kruskall-Wallis test followed by Tukey's post-tests to identify changes between stages of the estrous cycle. Masses were considered differentially abundant between groups with a P-value < 0.05. Hierarchical clustering of differential masses was performed using the gplot (v 3.0.1) and RcolorBrewer (v 1.1-2) packages of the R software. Principal Component Analysis (PCA) of differential masses was performed using the FactoMineR package (v1.41) of the R software. The fold-changes were calculated for each mass as ratios between the mean normalized intensity values at two stages.

2.4. Lipid identification by high-resolution tandem mass spectrometry (HR-MS/MS)

Total lipids were extracted from OF according to the 'Bligh and Dyer' method. A pool of 160 µL of OF (made with an equivalent volume (20 µL) of each stage and side) was mixed with 50 µL of methanol (MetOH), vortexed during 60 s then put on ice for 2 h. Chloroform (210 µL) was added then the samples were mixed, centrifuged (2000 g, 20 s), sonicated on ice for 10 min, mixed with 35 µL of water (Optima LC/MS grade, Fisher Scientific, Illkirch, France) and put on ice for 10 min. The samples were then centrifuged at 2500 g for 10 min, allowing to separate the aqueous phase (polarized lipids) from the organic phase (non-polarized lipids). The aqueous phase was then dried by a SpeedVac system (SPD 1010-230, Thermo Savant Eletronic, France) and pellets were stored in liquid nitrogen before analysis. Extracts were re-solubilized in 10 µL of methanol for the positive mode and in 10 µL of ammonium acetate at 20 mM in methanol for the negative mode, then analyzed on a dual linear ion trap Fourier Transform Mass Spectrometer (FT-MS) LTQ Orbitrap Velos (Thermo Fisher Bremen, Germany) using the Xcalibur software (version 2.1, Thermo Fisher Scientific, Bremen,

Germany), as previously described [25]. Briefly, FT-MS spectra were acquired using the profile mode in the 400–2000 *m*/*z* mass range, and the FT-MS/MS spectrum using high-energy collisional dissociation (HCD) fragmentation ion mode. Target resolution was set at 100,000 for FT-MS and FT-MS/MS analysis. The selected precursor width for fragmentation was 1.5 *m*/*z*. FT-MS and FT-MS/MS spectra were acquired, over 10 min, in triplicate, using different collision energy levels (20 to 60 keV with a step of 5 keV for the positive mode, 30 and 40 keV for the negative mode). Data were collected using spectral stitching technique as a series of 100-*m*/*z* wide windows that overlap by 5 *m*/*z*. Peaks were considered when >500 counts.

2.5. Validation and analysis of HR-MS/MS data

FT-MS and FT-MS/MS data were converted to Mascot generic format (MGF) using the Proteome Discoverer (version 1.4, ThermoFisher Scientific, San Jose, USA) and the LipidMatch softwares [27]. Each automatic lipid identification performed by LipidMatch (mass accuracy of 0.05 m/z for precursor and 50 ppm for fragment ions, score = level 1) was validated using LipidBlast 2.0 software [28]. For phospholipids and sphingolipids, all identifications with a Rev-Dot score >800 were accepted considering the presence of specific fragments ions error mass accuracy of 0.8 Da. For each identified lipid, theoretical mass (error mass accuracy < 0.05 Da) and formula were obtained through interrogation of the LIPID MAPS database (http://www.lipidmaps.org). Masses highlighted by the hierarchical clustering were annotated with the LIPID MAPS database using the same criteria.

3. Results

3.1. Lipid species identified in the OF

Using MALDI-MS, the lipid profile of the OF retrieved a total of 274 masses in the 400-1000 m/z (ratio of mass to charge, equivalent to Da) range, annotated mainly as phosphatidylcholines (PC), lysoPC (LPC), phosphatidylethanolamine (PE), lysoPE (LPE) and sphingomyelins (SM). One representative spectrum is shown in Fig. 1 and all the annotations are listed in Suppl. Table 1. By HR-MS/MS, 63 lipid species were identified, corresponding to cholesterol, 16 species of PC, one LPC, 27 PE, 11 LPE, one phosphatidylinositol (PI), one phosphatidylserine (PS), one SM and four L-carnitines (CAR). The observed and theoretical masses, name and formula of all identified lipid molecules are in Suppl. table 2.

3.2. Changes in lipid profiles according to the stage of the estrous cycle

For a given stage of the estrous cycle, the OF lipid profiles did not differ between ipsilateral and contralateral OF. However, the lipid profiles varied according to the stage of the estrous cycle: in total, 127 and 96 masses were differentially abundant between stages in ipsilateral and contralateral OF, respectively ($P < 0.05$; see all differential masses with p-values and fold-changes in Supplementary table 2). The PCA on differential masses in the ipsilateral OF clearly separated the Pre-ov stage from the others (Fig. 2). The highest proportion of differential masses were identified in the Pre-ov *vs*. Mid-lut comparison (75.4% of differential masses; 70 masses more and 34 less abundant at Pre-ov), followed in decreasing order by Pre-ov *vs*. Late-lut (52.9%; 44 more and 29 less abundant at Pre-ov), Pre-ov *vs*. Post-ov (31.9%; 21 more and 23 less abundant at Pre-ov), Post-ov *vs*. Mid-lut (13.8%; 17 more and 2 less abundant at Post-ov) and Post-ov *vs*. Late-lut (10.1%; 17 more and 2 less abundant at Post-ov; Fig. 3). The Mid-lut *vs*. Late-lut comparison showed no significant difference. The proportion and distribution of differential masses in the contralateral OF were similar (Suppl. Fig. 1).

3.3. Changes in lipid molecules according to the stage of the estrous cycle

The hierarchical clustering of differential masses in the ipsilateral OF confirmed the specificity of the Pre-ov stage and outlined two clusters of differentially abundant masses at

Pre-ov compared with the other stages of the estrous cycle (Fig. 4). After identification or annotation of these particular masses, a first cluster with more abundant lipids at Pre-ov than at other stages included molecules of PE, SM and LPC while a second cluster of masses, less abundant at Pre-ov than at other stages, included molecules of CAR and LPC. This second cluster of less abundant masses at Pre-ov was the only one identified in the contralateral oviduct (Suppl. Fig. 2).

The differential masses identified by HR-MS/MS included three molecules of CAR (18:2, 20:2 and 20:3), all decreased in abundance at Pre-ov compared with Post-ov, Mid-lut and Late-lut ($P<0.05$; Fig. 5). On the opposite, all identified molecules of PE (36:4, 36:5, 38:2, 38:3, 38:4, 38:5, 39:6, 40:4 (that could be also attributed to PC(37:4), 40:5 and 40:6), PC (34:1, 36:3, 36:4, 38:3, 40:5) and SM (d42:1) were increased at Pre-ov compared with at least one of the other stages (Post-ov, Mid-lut and/or Late-lut). In addition, five molecules of PE (36:5, 38:3, 39:6, 40:4 and 40:5) and two of PC (34:1 and 36:3) were increased at Post-ov compared with Mid-lut and/or Late-lut ($P<0.05$; Fig. 5).

4. Discussion

In order to better understand the regulation of lipid secretion within the tubal fluid, a global lipidomic approach using MALDI-MS and HR-MS/MS was applied. For the first time, a wide range of lipid compounds were identified by mass spectrometry in the bovine OF. The lipid profiles in the OF showed no variation between the sides relative to ovulation but changed significantly according to the stage of the estrous cycle, notably between the pre-ovulatory stage and the luteal phase.

Although they constitute crucial substrates for spermatozoa and developing embryos, lipids in the mammalian oviduct have not been studied in detail [3]. Most previous studies conducted on the bovine OF made no distinction between the lipid compounds that were

quantified [5, 21, 22]. In the present study, 63 lipid species, mostly phospholipids, were identified by HR-MS/MS. Our findings show that the tubal secretions contain a complex mixture of cholesterol, glycerophospholipids (PC, PE, PI and PS), lysophospholipids (LPC, LPE), sphingomyelins and carnitines. Carnitines (β-hydroxy-γ-trimethylammonium butyrate) are quaternary amines required for the transfer of long-chain fatty acids to mitochondria for subsequent β-oxidation [29]. One previous study from Killian *et al*. identified various glycerophospholipids and lysophospholipids in the bovine OF after separation by liquid chromatography, digestion and analysis of inorganic phosphorus [4]. Using high resolution MS, a more recent study identified molecules of PC, SM and PE in oviductal sections from *Bos indicus* cows [23]. However, ceramides and diacylglycerols were also identified in the latter while PI, PS, LPC, LPE and CAR were identified only in the present study. These discrepancies in identified lipids could be due to differences in MS techniques but may also reflect difference between bovine species, oviduct compartment (whole tissue section *vs*. OF) and region (ampulla *vs*. whole oviduct) studied.

The source of phospholipids and mechanism of their accumulation in the OF remain uncertain. Epithelial cells and cellular debris were eliminated from the OF by centrifugation before analysis, however, part of epithelial cells collected together with the OF may have released their content at the time of collection. Furthermore, the OF contains microvesicles and exosomes, both known as extracellular vesicles (EV) [30], that may originate from the oviduct epithelium [31] as well as from the pre-ovulatory follicle [32]. A large part of microvesicles (100 to 1000 nm in diameter) initially present in the OF were probably eliminated in the 12 000 g pellet. However, all exosomes (30 to 150 nm in diameter), typically collected by ultracentrifugation [9], were included in the present analysis. The exact lipid composition of EVs in the OF is not known but these submicroscopic vesicles have a lipid composition rich in phospholipids, similar to those in the cell membrane [8] and exosomes are

generally enriched in cholesterol, SM, glycosphingolipids and PS [33]. Thus, the lipids identified in this study may originate from either the cytoplasm of oviduct epithelial cells and/or the EV released in the OF.

The MALDI-MS profiling of a total of 136 OF samples collected at four different stages of the estrous cycle and in both sides relative to ovulation (17 females per stage and side) allowed us to identify the stage in the estrous cycle as a major factor of regulation of the OF phospholipid content. By contrast, the side of ovulation had no significant effect on the lipid profiles through the estrous cycle. We cannot exclude variation in other OF lipid compounds (triglycerides, ceramides, diacylglycerols and phosphatidic acid) that were not detected by MALDI-MS. To our knowledge, this is the first study comparing the lipid compounds in the oviduct according to the side of ovulation in a mono-ovular species. Many studies comparing the OF composition between the two sides relative to ovulation, including those from our laboratory, reported differences in steroid hormones and protein content in the OF [18, 19]. However, similar to the present work, previous studies in the field of metabolomics failed to evidence differences in the concentrations of amino acids and energy substrates between ipsilateral and contralateral oviducts [34-37]. In accordance, in a recent study using nuclear magnetic resonance (NMR) spectroscopy, of the 26 metabolites quantified in the OF, the concentrations of 14 metabolites varied according to the stage of the cycle while only five were affected by the side of ovulation with low extent of changes between sides [17]. In the present study, the similarity in lipid profiles observed between the two sides of ovulation does not support the hypothesis of a contribution of the pre-ovulatory follicle to the lipid content of the OF, in particular at Post-ov.

Interestingly, the highest proportions of differentially abundant lipids were identified when comparing the Pre-ov and Mid-lut or Pre-ov and Late-lut stages in both sides relative to ovulation. In a previous study, we reported important fluctuations in the concentrations of the

290 ovarian steroid hormones P4 and E2 according to the stage of the estrous cycle in the bovine
291 OF [19]. In accordance with fluctuations observed in the circulating plasma, oviductal levels
292 of P4 were highest at Mid-lut and Late-lut stages and lowest at Pre-ov (means of 120.3 and
293 76.7 *vs*. 6.3 ng/mL, respectively) whereas E2 reached maximal levels at Pre-ov and minimum
294 levels at Mid- and Late-lut (means of 290.5 vs. 86.3 and 44.0 pg/ml, respectively) [19].
295 Therefore, lipid masses more abundant at Pre-ov than at other stages paralleled the circulating
296 and topical levels of E2 whereas more abundant masses at Mid-Lut and Late-lut paralleled
297 those of P4, supporting the hypothesis of some endocrine regulation of the lipid composition
298 of the OF. In accordance, the total quantity of phospholipids in the OF were reported to vary
299 between luteal and non-luteal phases of the cycle in cows [4, 5] and buffalos [22].
300 Furthermore, in a *Bos indicus* model with contrasted circulating levels of E2 before ovulation
301 and of P4 after ovulation, variation in the phospholipid profiles monitored by MALDI-MS
302 were reported in the oviduct at Day 4 and in the uterus at Days 4 and 7 post-ovulation [23].
303 Some of the differential lipid masses identified in the latter (for example m/z 782.6 PC (36:4)
304 and m/z 836.6 PC (40:5)) were also found differentially abundant between Pre-ov and Mid-lut
305 or Late-lut in the present study, leading to the hypothesis that a specific phospholipid profile
306 is generated in the bovine genital secretions according to the steroid hormonal environment.

307 Not much is known about the mechanisms by which P4 and E2 may regulate the lipid
308 content in the OF. Nuclear receptors for P4 and E2 have been reported in the bovine oviduct
309 epithelium [38]. Membrane receptors for P4 are also expressed in bovine oviduct epithelial
310 cells [39], raising the possibility of a non-genomic action of this hormone in the oviduct
311 epithelium. Steroid hormones might modulate the rate of release of EV by the oviduct
312 epithelial cells and thus modulate the accumulation of vesicular phospholipids into the OF.
313 However, in a recent study, no difference in the concentration and size of bovine oviduct EVs
314 have been recorded between stages in the estrous cycle [40]. Alternatively, E2 and P4 may

315 modulate the synthesis of proteins involved in the production, transport and cellular export of
316 lipids and fatty acids. Accordingly, number of genes involved in the lipid biosynthesis process
317 (including for instance *LPIAT1*, *PIGW*, *CPT1B* and *LPCAT4* coding for
318 lysophosphatidylinositol acyltransferase 1, phosphatidylinositol-glycan biosynthesis protein,
319 carnitine O-palmitoyltransferase 1, and lysophospholipid acyltransferase, respectively) were
320 differentially expressed in oviduct epithelial cells from zebuine females with contrasted
321 periovulatory concentrations of ovarian steroid hormones [41]. Also, various proteins
322 involved in lipid metabolism were reported to vary in abundance according to the stage of the
323 cycle in the bovine OF [18]. In particular, fatty acid synthase (FASN) was among the most
324 differentially abundant proteins between the Pre-ov and Post-ov stages. Nevertheless,
325 mechanistic studies designed to understand the action of the endocrine environment on the
326 lipid content of the oviduct are needed.

327 Spermatozoa enter the oviduct during the pre-ovulatory period and can be stored on
328 site for hours to days before ovulation, at which time sperm capacitation and fertilization
329 occur [42]. Spermatozoa are rich in very-long-chain polyunsaturated fatty acids and are highly
330 sensitive to the lipid environment to which they are exposed [43]. Exogenous
331 glycerophospholipids can be incorporated within the membrane of mammalian spermatozoa
332 [10, 44]. Several phospholipids including identified PC and LPC as well as carnitine
333 molecules were found modulated in abundance during the periovulatory period compared
334 with the other stages of the estrous cycle. Exogenous PC and LPC have a destabilizing effect
335 on sperm membrane and were able to induce bull sperm capacitation and acrosome reaction
336 within minutes [11, 45, 46]. By contrast, exogenous L-carnitine was reported to inhibit sperm
337 capacitation and acrosome reaction, possibly through a stabilization of sperm membrane
338 phospholipids [47-49]. The abundance of several molecules of CAR in the OF was highly
339 decreased at Pre-ov and increased just after ovulation. It is tempting to speculate that this

specific pre-ovulatory oviductal environment plays a role in the prevention of premature capacitation before ovulation. However, numerous phospholipids were also upregulated in abundance at Pre-ov and the exact role of the complex lipidomic milieu identified at this stage on spermatozoa remain largely unknown.

Among phospholipids found more abundant during the periovulatory period compared with the luteal phase, the PC 34:1 (m/z 760.6) was previously reported as one of the most abundant phospholipid identified by MALDI-MS in bovine blastocysts produced either *in vivo* or *in vitro* [13, 50]. Furthermore, the m/z 754.6, 756.6, 768.6 and 780.6, annotated as molecules of PC and PE and observed as more abundant at Pre-ov compared with Mid-lut and/or Late-lut, have been reported to increase in abundance in bovine embryos at stages of development that physiologically occur in the oviduct [12]. Thus, specific phospholipid profiles fitting with the needs of the developing embryo seemed to appear in the OF during the periovulatory period. However, functional roles of the phospholipids with regulated abundance during the periovulatory period deserve further studies.

5. Conclusions

The periovulatory period of the estrous cycle displayed a highly specific OF lipidomic profile compared with that in the luteal phase, pointing out a probable regulatory role of ovarian steroid hormones in the regulation of the oviduct lipid content. The mechanisms by which phospholipids accumulate in the oviductal lumen and their exact roles on gametes and embryo require further investigations.

Acknowledgments

The authors are grateful to Thierry Delpech, Albert Arnout and Justine Saulnier for their help in the collection of biological samples, and to Marc Chodkiewicz for editing the manuscript.

Funding

This research was funded by INRA. CB was funded by the French cooperative UNION EVOLUTION and the Association Nationale de la Recherche et de la Technologie (ANRT) as recipient of the Convention Industrielle de Formation par la Recherche no 2017/0684. The high resolution mass spectrometer was funded (SMHART project n°3069) by the European Regional Development Fund (ERDF), the Conseil Régional du Centre, the French National Institute for Agricultural Research (INRA) and the French National Institute of Health and Medical Research (Inserm). The funding sources had no involvement in the study design, analysis of data and publication.

Conflict of interest

The authors declare they have no conflict of interest.

References

[1] Leese HJ, Hugentobler SA, Gray SM, Morris DG, Sturmey RG, Whitear SL, et al. Female reproductive tract fluids: composition, mechanism of formation and potential role in the developmental origins of health and disease. Reprod Fertil Dev. 2008;20:1-8.

[2] Leese HJ, Tay JI, Reischl J, Downing SJ. Formation of Fallopian tubal fluid: role of a neglected epithelium. Reproduction. 2001;121:339-46.

[3] Menezo Y, Guerin P, Elder K. The oviduct: a neglected organ due for re-assessment in IVF. Reprod Biomed Online. 2015;30:233-40.

[4] Killian GJ, Chapman DA, Kavanaugh JF, Deaver DR, Wiggin HB. Changes in phospholipids, cholesterol and protein content of oviduct fluid of cows during the oestrous cycle. J Reprod Fertil. 1989;86:419-26.

386 [5] Grippo AA, Anderson SH, Chapman DA, Henault MA, Killian GJ. Cholesterol,
387 phospholipid and phospholipase activity of ampullary and isthmic fluid from the bovine
388 oviduct. J Reprod Fertil. 1994;102:87-93.
389 [6] Jordaens L, Van Hoeck V, De Bie J, Berth M, Marei WFA, Desmet KLJ, et al. Non-
390 esterified fatty acids in early luteal bovine oviduct fluid mirror plasma concentrations: An ex
391 vivo approach. Reprod Biol. 2017;17:281-4.
392 [7] Eyster KM. The membrane and lipids as integral participants in signal transduction: lipid
393 signal transduction for the non-lipid biochemist. Adv Physiol Educ. 2007;31:5-16.
394 [8] Kastelowitz N, Yin H. Exosomes and microvesicles: identification and targeting by
395 particle size and lipid chemical probes. Chembiochem. 2014;15:923-8.
396 [9] Record M, Silvente-Poirot S, Poirot M, Wakelam MJO. Extracellular vesicles: lipids as
397 key components of their biogenesis and functions. J Lipid Res. 2018;59:1316-24.
398 [10] Evans RW, Setchell BP. Association of exogenous phospholipids with spermatozoa. J
399 Reprod Fertil. 1978;53:357-62.
400 [11] Wheeler MB, Seidel GE, Jr. Capacitation of bovine spermatozoa by lysophospholipids
401 and trypsin. Gamete Res. 1989;22:193-204.
402 [12] Sudano MJ, Rascado TD, Tata A, Belaz KR, Santos VG, Valente RS, et al. Lipidome
403 signatures in early bovine embryo development. Theriogenology. 2016;86:472-84 e1.
404 [13] Sudano MJ, Santos VG, Tata A, Ferreira CR, Paschoal DM, Machado R, et al.
405 Phosphatidylcholine and sphingomyelin profiles vary in Bos taurus indicus and Bos taurus
406 taurus in vitro- and in vivo-produced blastocysts. Biol Reprod. 2012;87:130.
407 [14] Desmet KL, Van Hoeck V, Gagne D, Fournier E, Thakur A, O'Doherty AM, et al.
408 Exposure of bovine oocytes and embryos to elevated non-esterified fatty acid concentrations:
409 integration of epigenetic and transcriptomic signatures in resultant blastocysts. BMC
410 Genomics. 2016;17:1004.

411 [15] Leao BC, Rocha-Frigoni NA, Cabral EC, Coelho MB, Ferreira CR, Eberlin MN, et al.
412 Improved embryonic cryosurvival observed after in vitro supplementation with conjugated
413 linoleic acid is related to changes in the membrane lipid profile. Theriogenology.
414 2015;84:127-36.
415 [16] Abe H, Yamashita S, Satoh T, Hoshi H. Accumulation of cytoplasmic lipid droplets in
416 bovine embryos and cryotolerance of embryos developed in different culture systems using
417 serum-free or serum-containing media. Mol Reprod Dev. 2002;61:57-66.
418 [17] Lamy J, Gatien J, Dubuisson F, Nadal-Desbarats L, Salvetti P, Mermillod P, et al.
419 Metabolomic profiling of bovine oviductal fluid across the oestrous cycle using proton
420 nuclear magnetic resonance spectroscopy. Reprod Fertil Dev. 2018;30:1021-8.
421 [18] Lamy J, Labas V, Harichaux G, Tsikis G, Mermillod P, Saint-Dizier M. Regulation of
422 the bovine oviductal fluid proteome. Reproduction. 2016;152:629-44.
423 [19] Lamy J, Liere P, Pianos A, Aprahamian F, Mermillod P, Saint-Dizier M. Steroid
424 hormones in bovine oviductal fluid during the estrous cycle. Theriogenology. 2016;86:1409-
425 20.
426 [20] Hunter RH. Components of oviduct physiology in eutherian mammals. Biol Rev Camb
427 Philos Soc. 2012;287:244-55.
428 [21] Ehrenwald E, Foote RH, Parks JE. Bovine oviductal fluid components and their potential
429 role in sperm cholesterol efflux. Mol Reprod Dev. 1990;25:195-204.
430 [22] Vecchio D, Neglia G, Di Palo R, Campanile G, Balestrieri ML, Giovane A, et al. Ion,
431 protein, phospholipid and energy substrate content of oviduct fluid during the oestrous cycle
432 of buffalo (Bubalus bubalis). Reprod Domest Anim. 2010;45:e32-9.
433 [23] Belaz KR, Tata A, Franca MR, Santos da Silva MI, Vendramini PH, Fernandes AM, et
434 al. Phospholipid Profile and Distribution in the Receptive Oviduct and Uterus During Early
435 Diestrus in Cattle. Biol Reprod. 2016;95:127.

436 [24] Rico C, Medigue C, Fabre S, Jarrier P, Bontoux M, Clement F, et al. Regulation of anti-
437 Mullerian hormone production in the cow: a multiscale study at endocrine, ovarian, follicular,
438 and granulosa cell levels. Biol Reprod. 2011;84:560-71.
439 [25] Bertevello PS, Teixeira-Gomes AP, Seyer A, Vitorino Carvalho A, Labas V, Blache MC,
440 et al. Lipid Identification and Transcriptional Analysis of Controlling Enzymes in Bovine
441 Ovarian Follicle. Int J Mol Sci. 2018;19.
442 [26] Gibb S, Strimmer K. MALDIquant: a versatile R package for the analysis of mass
443 spectrometry data. Bioinformatics. 2012;28:2270-1.
444 [27] Koelmel JP, Kroeger NM, Ulmer CZ, Bowden JA, Patterson RE, Cochran JA, et al.
445 LipidMatch: an automated workflow for rule-based lipid identification using untargeted high-
446 resolution tandem mass spectrometry data. BMC Bioinformatics. 2017;18:331.
447 [28] Kind T, Liu KH, Lee DY, DeFelice B, Meissen JK, Fiehn O. LipidBlast in silico tandem
448 mass spectrometry database for lipid identification. Nat Methods. 2013;10:755-8.
449 [29] Longo N, Frigeni M, Pasquali M. Carnitine transport and fatty acid oxidation. Biochim
450 Biophys Acta. 2016;1863:2422-35.
451 [30] Alminana C, Corbin E, Tsikis G, Alcantara-Neto AS, Labas V, Reynaud K, et al.
452 Oviduct extracellular vesicles protein content and their role during oviduct-embryo cross-talk.
453 Reproduction. 2017;154:153-68.
454 [31] Lopera-Vasquez R, Hamdi M, Fernandez-Fuertes B, Maillo V, Beltran-Brena P, Calle A,
455 et al. Extracellular Vesicles from BOEC in In Vitro Embryo Development and Quality. PLoS
456 One. 2016;11:e0148083.
457 [32] Hung WT, Navakanitworakul R, Khan T, Zhang P, Davis JS, McGinnis LK, et al. Stage-
458 specific follicular extracellular vesicle uptake and regulation of bovine granulosa cell
459 proliferation. Biol Reprod. 2017;97:644-55.

460 [33] Skotland T, Hessvik NP, Sandvig K, Llorente A. Exosomal lipid composition and the
461 role of ether lipids and phosphoinositides in exosome biology. J Lipid Res. 2019;60:9-18.
462 [34] Kenny DA, Humpherson PG, Leese HJ, Morris DG, Tomos AD, Diskin MG, et al. Effect
463 of elevated systemic concentrations of ammonia and urea on the metabolite and ionic
464 composition of oviductal fluid in cattle. Biol Reprod. 2002;66:1797-804.
465 [35] Hugentobler SA, Diskin MG, Leese HJ, Humpherson PG, Watson T, Sreenan JM, et al.
466 Amino acids in oviduct and uterine fluid and blood plasma during the estrous cycle in the
467 bovine. Mol Reprod Dev. 2007;74:445-54.
468 [36] Hugentobler SA, Humpherson PG, Leese HJ, Sreenan JM, Morris DG. Energy substrates
469 in bovine oviduct and uterine fluid and blood plasma during the oestrous cycle. Mol Reprod
470 Dev. 2008;75:496-503.
471 [37] Elhassan YM, Wu G, Leanez AC, Tasca RJ, Watson AJ, Westhusin ME. Amino acid
472 concentrations in fluids from the bovine oviduct and uterus and in KSOM-based culture
473 media. Theriogenology. 2001;55:1907-18.
474 [38] Ulbrich SE, Kettler A, Einspanier R. Expression and localization of estrogen receptor
475 alpha, estrogen receptor beta and progesterone receptor in the bovine oviduct in vivo and in
476 vitro. J Steroid Biochem Mol Biol. 2003;84:279-89.
477 [39] Saint-Dizier M, Sandra O, Ployart S, Chebrout M, Constant F. Expression of nuclear
478 progesterone receptor and progesterone receptor membrane components 1 and 2 in the
479 oviduct of cyclic and pregnant cows during the post-ovulation period. Reprod Biol
480 Endocrinol. 2012;10:76.
481 [40] Alminana C, Tsikis G, Labas V, Uzbekov R, da Silveira JC, Bauersachs S, et al.
482 Deciphering the oviductal extracellular vesicles content across the estrous cycle: implications
483 for the gametes-oviduct interactions and the environment of the potential embryo. BMC
484 Genomics. 2018;19:622.

485 [41] Gonella-Diaza AM, Andrade SC, Sponchiado M, Pugliesi G, Mesquita FS, Van Hoeck
486 V, et al. Size of the Ovulatory Follicle Dictates Spatial Differences in the Oviductal
487 Transcriptome in Cattle. PLoS One. 2015;10:e0145321.
488 [42] Coy P, Garcia-Vazquez FA, Visconti PE, Aviles M. Roles of the oviduct in mammalian
489 fertilization. Reproduction. 2012;144:649-60.
490 [43] Lenzi A, Picardo M, Gandini L, Dondero F. Lipids of the sperm plasma membrane: from
491 polyunsaturated fatty acids considered as markers of sperm function to possible scavenger
492 therapy. Hum Reprod Update. 1996;2:246-56.
493 [44] Ferreira G, Costa C, Bassaizteguy V, Santos M, Cardozo R, Montes J, et al. Incubation of
494 human sperm with micelles made from glycerophospholipid mixtures increases sperm
495 motility and resistance to oxidative stress. PLoS One. 2018;13:e0197897.
496 [45] Ehrenwald E, Parks JE, Foote RH. Cholesterol efflux from bovine sperm. I. Induction of
497 the acrosome reaction with lysophosphatidylcholine after reducing sperm cholesterol. Gamete
498 Res. 1988;20:145-57.
499 [46] Therien I, Manjunath P. Effect of progesterone on bovine sperm capacitation and
500 acrosome reaction. Biol Reprod. 2003;69:1408-15.
501 [47] Deana R, Indino M, Rigoni F, Foresta C. Effect of L-carnitine on motility and acrosome
502 reaction of human spermatozoa. Arch Androl. 1988;21:147-53.
503 [48] Longobardi V, Salzano A, Campanile G, Marrone R, Palumbo F, Vitiello M, et al.
504 Carnitine supplementation decreases capacitation-like changes of frozen-thawed buffalo
505 spermatozoa. Theriogenology. 2017;88:236-43.
506 [49] Aliabadi E, Jahanshahi S, Talaei-Khozani T, Banaei M. Comparison and evaluation of
507 capacitation and acrosomal reaction in freeze-thawed human ejaculated spermatozoa treated
508 with L-carnitine and pentoxifylline. Andrologia. 2018;50.

509 [50] Tata A, Sudano MJ, Santos VG, Landim-Alvarenga FD, Ferreira CR, Eberlin MN.

510 Optimal single-embryo mass spectrometry fingerprinting. J Mass Spectrom. 2013;48:844-9.

511

512

513 **Figure legends**

514 **Fig. 1.** Representative lipid profile obtained by MALDI-MS in the positive ion-mode on
515 bovine OF at the Pre-ov stage of the estrous cycle.

516 **Fig. 2.** Principal component analysis of differentially abundant lipid masses identified across
517 the estrous cycle in the oviductal fluid ipsilateral to ovulation. Each spot represents one
518 biological replicate (n=17 samples per stage). Each ellipse encloses 80 % of spots for each
519 stage. The square in each ellipse represents the mean of data for a given stage. Green
520 symbols: post-ovulatory stage; red: mid-luteal phase; black: late luteal stage; blue: pre-
521 ovulatory stage of the estrous cycle.

522 **Fig. 3.** Distribution of differentially abundant lipid species when comparing Pre-ov (**A**) and
523 Post-ov (**B**) with other stages of the estrous cycle in the OF ipsilateral to ovulation. Numbers
524 of identified masses and molecular species are indicated for all subgroups. The not
525 represented Mid-lut *vs.* Late-lut comparison retrieved no difference.

526 **Fig. 4.** Heatmap representation of hierarchical clustering of the 127 differentially abundant
527 lipid masses identified across the estrous cycle in the OF ipsilateral to ovulation. Each line
528 corresponds to one molecular mass. For a given stage and mass, green lines represent higher
529 abundance while red lines represent lower abundance compared with other stages. Black lines
530 represent is the median abundance values. The proximity between the stages and lipid profiles
531 are shown by the hierarchical trees on the top and left, respectively. The Cluster 1 identified
532 includes masses more abundant at the pre-ovulatory stage (Pre-ov) compared with the post-
533 ovulatory (Post-ov), mid- (Mid-lut) and late luteal (Late-lut) phases of the estrous cycle while
534 the Cluster 2 includes masses less abundant at Pre-ov than at other stages. NA: no annotation
535 nor identification.

536 **Fig. 5.** Changes in relative abundance of identified lipid molecules according to the stage of
537 the estrous cycle in the OF ipsilateral to ovulation. Different letters indicate significant
538 differences ($P<0.05$).

539

540

541

542

Legends of supplementary materials

Supplementary Table 1. List of all differentially abundant masses in paired comparisons between stages of the estrous cycle in the OF ipsilateral and contralateral to ovulation with related p-values and ratios. Annotations were obtained through LIPID MAPS database search.

Supplementary Table 2. List of all lipid species identified by HR-MS/MS in the OF and mode of identification. The theoretical mass and formula were obtained through LIPID MAPS database search. Right columns indicate differences in abundance between the stages when a significant effect of the stage was identified ($P<0.05$).

Supplementary Figure 1. Distribution of differentially abundant lipid species when comparing Pre-ov (**A**) and Post-ov (**B**) with other stages of the estrous cycle in the OF contralateral to ovulation. Numbers of identified masses are indicated for all subgroups. The not represented Mid-lut *vs*. Late-lut comparison retrieved no difference.

Supplementary Figure 2. Heatmap representation of hierarchical clustering of the 96 differentially abundant lipid masses identified across the estrous cycle in the OF contralateral to ovulation. Each line corresponds to one molecular mass. For a given stage and mass, green lines represent higher abundance while red lines represent lower abundance compared with other stages. Black lines represent is the median abundance values. The proximity between the stages and lipid profiles are shown by the hierarchical trees on the top and left, respectively. The cluster identified includes masses less abundant at Pre-ov than at other stages. NA: no annotation nor identification.

Figure 1

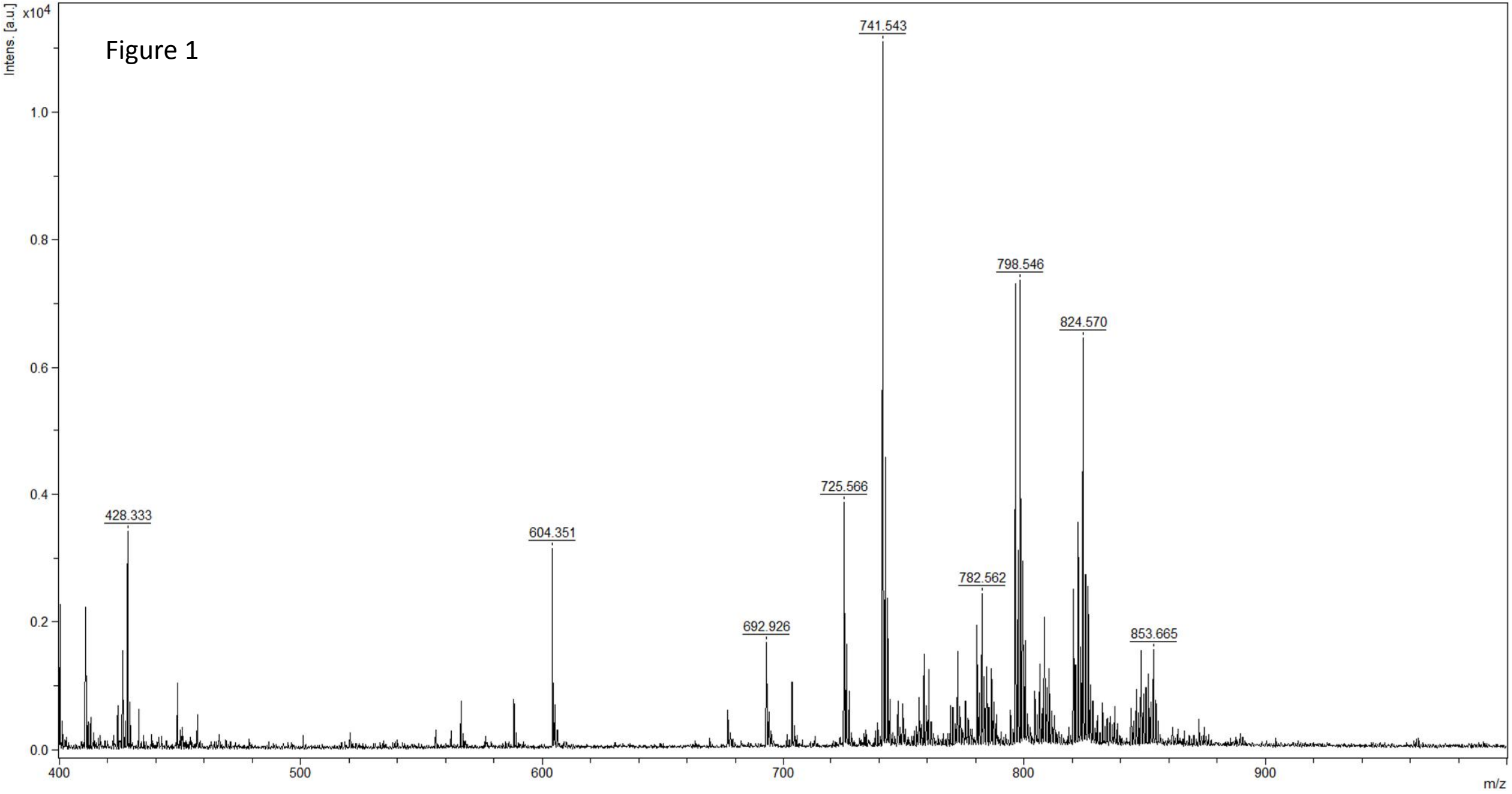
Intens. [a.u.]
x10^4
1.0
0.8
0.6
0.4
0.2
0.0
400
500
600
700
800
900
m/z
741.543
798.546
824.570
725.566
428.333
604.351
782.562
692.926
853.665

Figure 2

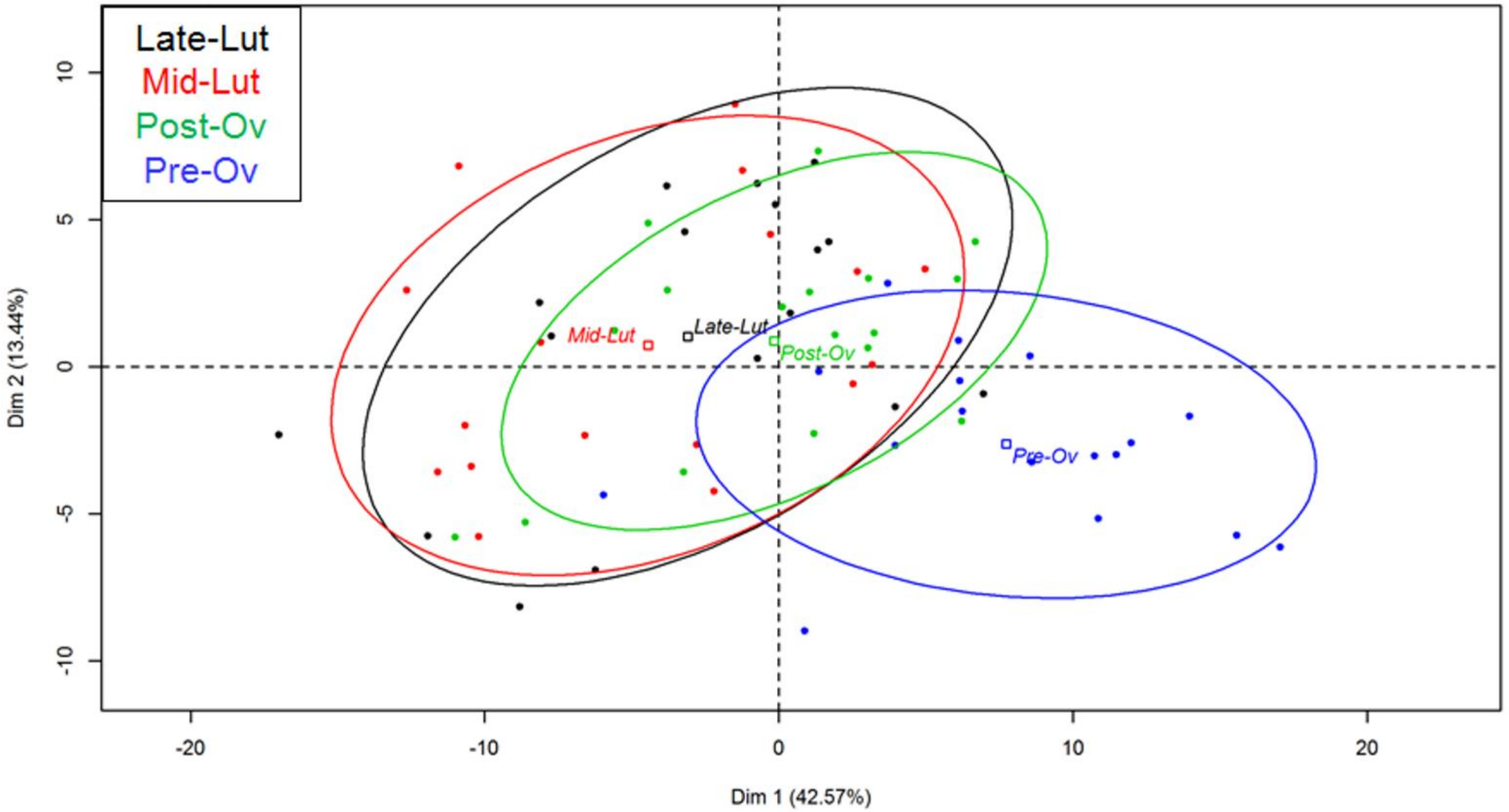
Late-Lut
Mid-Lut
Post-Ov
Pre-Ov
Mid-Lut
Late-Lut
Post-Ov
Pre-Ov
Dim 2 (13.44%)
Dim 1 (42.57%)
10
5
0
-5
-10
-20
-10
0
10
20

Figure 3

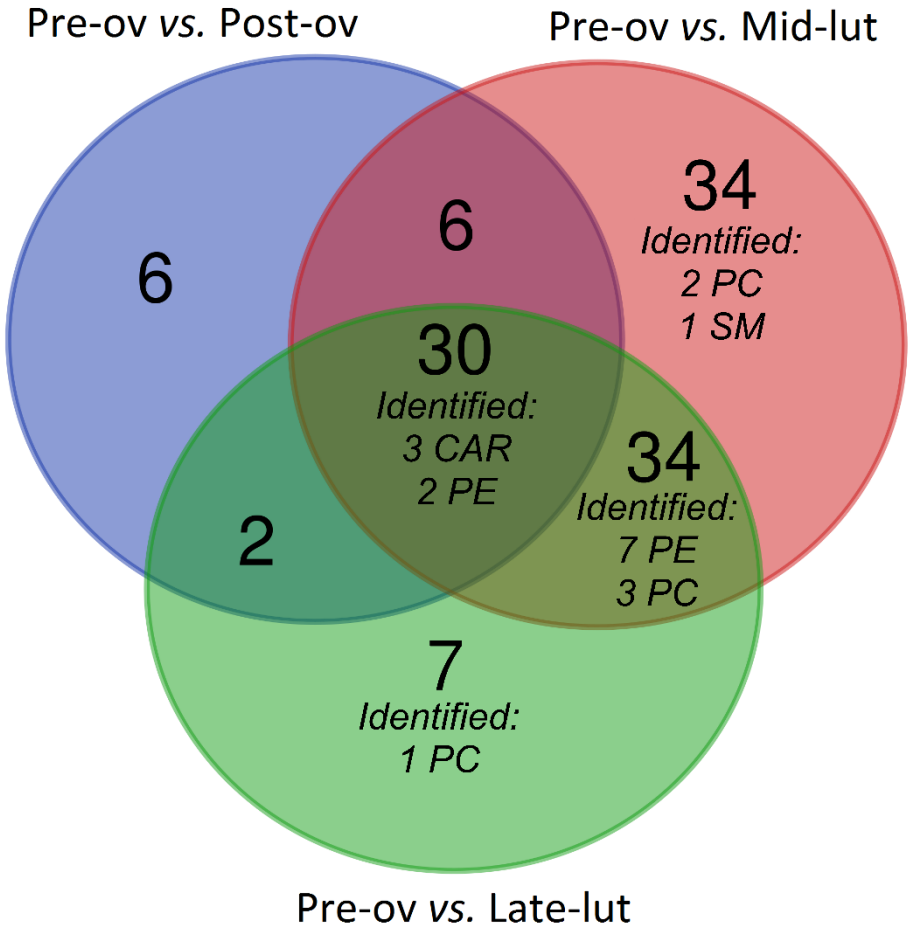
Pre-ov *vs.* Post-ov
Pre-ov *vs.* Mid-lut
6
6
34
Identified:
2 PC
1 SM
30
Identified:
3 CAR
2 PE
34
Identified:
7 PE
3 PC
2
7
Identified:
1 PC
Pre-ov *vs.* Late-lut

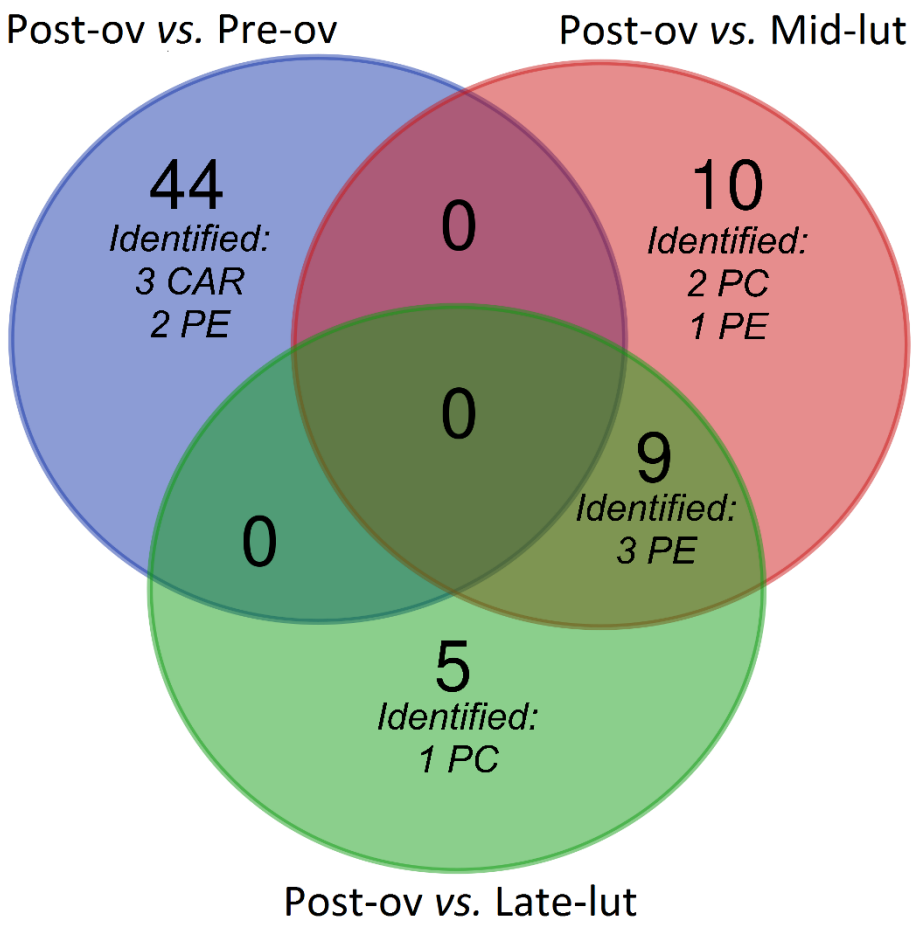
Post-ov *vs.* Pre-ov
Post-ov *vs.* Mid-lut
44
Identified:
3 CAR
2 PE
0
10
Identified:
2 PC
1 PE
0
0
9
Identified:
3 PE
5
Identified:
1 PC
Post-ov *vs.* Late-lut

Figure 4

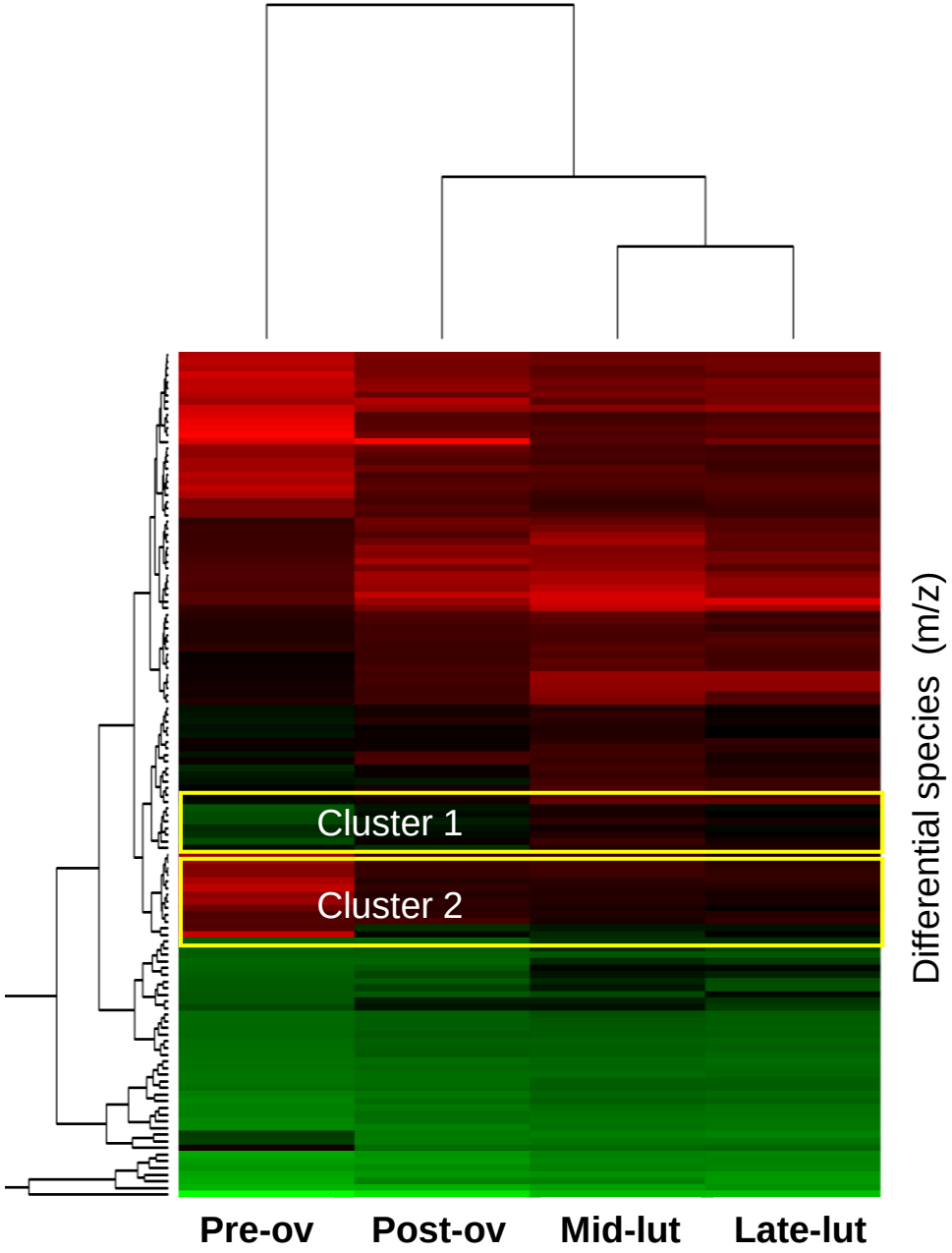

Cluster 1

Differences between stages	Mass (m/z)	Lipid	Identification or annotation
Pre-ov > Post-ov, Mid-lut & Late-lut	534,33	LPC(19:2) [M+H]+	Annotated
	739,55	SM(35:1) [M+Na]+	Annotated
	740,55	PE(36:4) [M+H]+	Identified
	740,62	NA	NA
	757,63	SM(38:2) [M+H]+	Annotated
	768,56	PE(38:4) [M+H]+	Identified
	795,62	SM(38:2) [M+K]+	Annotated

Cluster 2

Differences between stages	Mass (m/z)	Lipid	Identification or annotation
Post-ov, Mid-lut & Late-lut > Pre-ov	400,03	NA	NA
	401,32	NA	NA
	414,35	CAR(17:0)	Annotated
	416,27	NA	NA
	416,33	CAR(16-OH)+H	Annotated
	424,35	CAR(18:2)	Annotated
	438,31	CAR(18:3-OH)	Annotated
	441,33	NA	NA
	442,36	CAR(18:1-OH)	Annotated
	448,25	LPC(11:0) [M+Na]+	Annotated
	448,32	CAR(20:4)	Annotated
	450,35	CAR(20:3)	Identified
	466,35	LPC(14:1) [M+H]+	Annotated

Figure 5

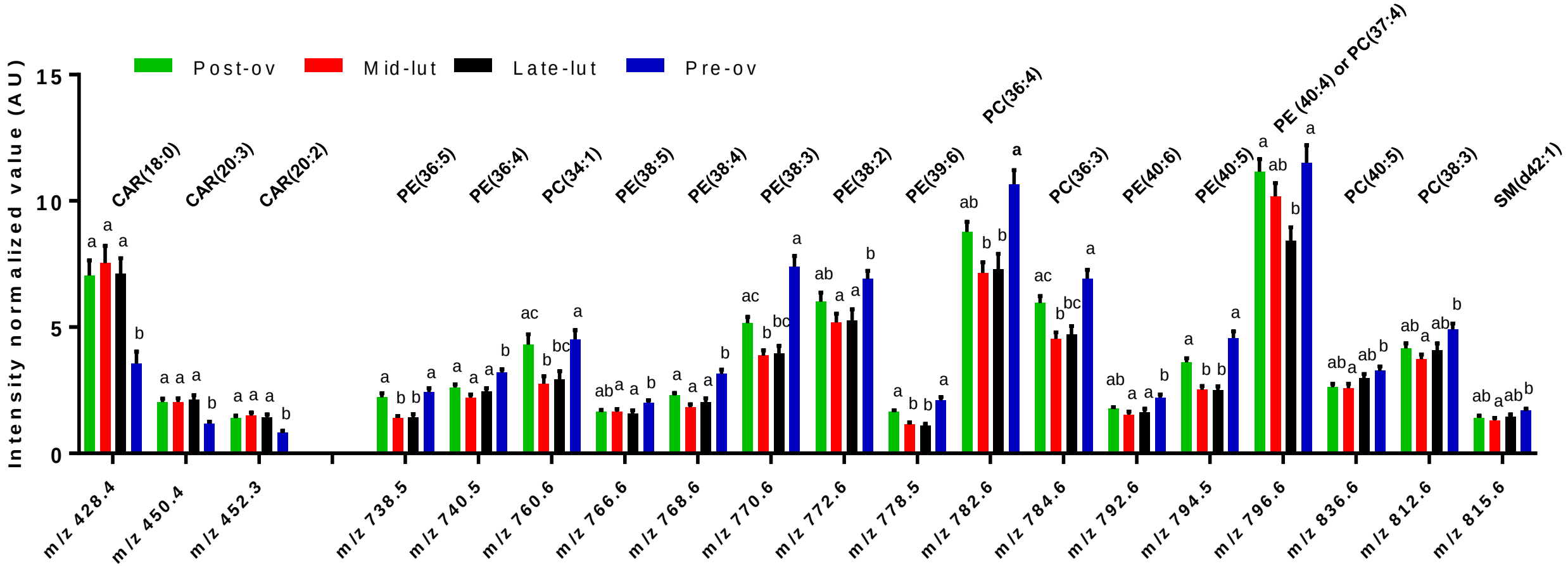
Post-ov
Mid-lut
Late-lut
Pre-ov
Intensity normalized value (AU)
15
10
5
0
CAR(18:0)
CAR(20:3)
CAR(20:2)
PE(36:5)
PE(36:4)
PC(34:1)
PE(38:5)
PE(38:4)
PE(38:3)
PE(38:2)
PE(39:6)
PC(36:4)
PC(36:3)
PE(40:6)
PE(40:5)
PE (40:4) or PC(37:4)
PC(40:5)
PC(38:3)
SM(d42:1)
m/z 428.4
m/z 450.4
m/z 452.3
m/z 738.5
m/z 740.5
m/z 760.6
m/z 766.6
m/z 768.6
m/z 770.6
m/z 772.6
m/z 778.5
m/z 782.6
m/z 784.6
m/z 792.6
m/z 794.5
m/z 796.6
m/z 836.6
m/z 812.6
m/z 815.6